NASA TECHNICAL MEMORANDUM

NASA TM X-2116

NASA TM X-2116



# PERFORMANCE OF A 10° CONICAL PLUG NOZZLE WITH A STOWED THRUST REVERSER AT MACH NUMBERS FROM 0 TO 2.0

*by Fred W. Steffen*

*Lewis Research Center*

*Cleveland, Ohio 44135*

NATIONAL AERONAUTICS AND SPACE ADMINISTRATION • WASHINGTON, D. C. • OCTOBER 1970

| 1. Report No. NASA TM X-2116 | 2. Government Accession No. | 3. Recipient's Catalog No. |
|---|---|---|
| 4. Title and Subtitle PERFORMANCE OF A 10° CONICAL PLUG NOZZLE WITH A STOWED THRUST REVERSER AT MACH NUMBERS FROM 0 TO 2.0 | | 5. Report Date October 1970<br>6. Performing Organization Code |
| 7. Author(s) Fred W. Steffen | | 8. Performing Organization Report No. E-5565 |
| 9. Performing Organization Name and Address Lewis Research Center National Aeronautics and Space Administration Cleveland, Ohio 44135 | | 10. Work Unit No. 720-03<br>11. Contract or Grant No.<br>13. Type of Report and Period Covered Technical Memorandum |
| 12. Sponsoring Agency Name and Address National Aeronautics and Space Administration Washington, D.C. 20546 | | 14. Sponsoring Agency Code |

15. Supplementary Notes

16. Abstract

Nozzles with two throat areas and two shroud lengths were tested. Compared to a hinged iris primary-plug nozzle without a reverser, the plug nozzle with the stowed thrust reverser had higher efficiency at subsonic cruise with the shroud retracted but lower efficiency at high pressure ratios with the shroud either retracted or extended. The stowed thrust reverser restricted corrected secondary-weight-flow ratio available from the free stream to 0.02 between Mach numbers of 0.4 and 1.1.

17. Key Words (Suggested by Author(s))

Propulsion
Nozzles
Thrust reversal

18. Distribution Statement

Unclassified - unlimited

| 19. Security Classif. (of this report) | 20. Security Classif. (of this page) | 21. No. of Pages | 22. Price* |
|---|---|---|---|
| Unclassified | Unclassified | 26 | $3.00 |

*For sale by the Clearinghouse for Federal Scientific and Technical Information
Springfield, Virginia 22151

# PERFORMANCE OF A 10° CONICAL PLUG NOZZLE WITH A STOWED THRUST REVERSER AT MACH NUMBERS FROM 0 TO 2.0

by Fred W. Steffen

Lewis Research Center

## SUMMARY

Air was used as the primary and secondary fluid. Two primary nozzles were used with two different shroud lengths. The smaller primary nozzle simulated afterburner-off operation at subsonic speeds when combined with the short shroud, and supersonic-cruise operation when combined with the long shroud. The larger primary nozzle simulated an afterburner-on acceleration geometry. Nozzle gross-thrust coefficients and pumping characteristics were measured.

The nozzle had a high gross-thrust coefficient at subsonic cruise (0.96 at $M_0 = 0.85$ and $\omega\sqrt{\tau} = 0.02$). At a Mach number of 1.97 and a nozzle pressure ratio of 26 with no secondary flow, the nozzle gross-thrust coefficient was 0.950, which was 2.3 percentage points less than that for a hinged iris primary-plug nozzle without a thrust reverser.

The stowed thrust reverser restricted the secondary flow to the extent that it would be impossible to obtain a corrected secondary-weight-flow ratio of 0.04 from the free stream below Mach 1.1. However, a corrected secondary-weight-flow ratio of 0.02 could be obtained from a free-stream source at most flight conditions.

## INTRODUCTION

In its current program in airbreathing propulsion, the Lewis Research Center is evaluating various nozzles appropriate for supersonic-cruise applications. One such nozzle being considered is the low-angle conical plug nozzle. Its performance has been reported in reference 1.

For some applications, the plug nozzle must also have reverse thrust capability. The particular thrust reverser design considered herein consists of a translating iris primary nozzle which can close against the plug surface. The entire jet is then exhausted in a forward direction through cascade boxes installed in the primary nozzle leaves. To

obtain the proper motion, the primary nozzle has an outer wall comprised of spherical sections. For subsonic operation, the primary nozzle forms a low-drag circular-arc boattail. For supersonic operation, the design permits the extension of a cylindrical shroud to contain the expansion of the exhaust gases.

This report presents the results of tests made with a wind tunnel model of a plug nozzle containing a stowed thrust reverser of the type just described. Where possible, the performance is compared to that reported in reference 1 for a hinged iris primary-plug nozzle without a thrust reverser.

Two primary nozzles were used with two different shroud lengths. The smaller primary nozzle simulated afterburner-off operation at subsonic speeds when combined with a short shroud and supersonic-cruise operation when combined with a long shroud. The larger primary nozzle simulated a geometry which would exist at afterburner-on power settings.

The tests were conducted in the Lewis Research Center 8- by 6-Foot Supersonic Wind Tunnel at Mach numbers from 0 to 2.0. At each Mach number, nozzle pressure ratio was varied around a typical value for a supersonic turbojet engine. Corrected secondary-weight-flow ratio was varied from 0 to 0.15. Room-temperature air was used as the primary and secondary fluid. Nozzle gross-thrust coefficients, nozzle efficiencies, and pumping characteristics were determined.

## SYMBOLS

A area

D drag

d model diameter

F jet thrust

M Mach number

P total pressure

p static pressure

r radius

T total temperature

W weight-flow rate

$\theta$ angular coordinate, measured clockwise from top while looking upstream

$\tau$ temperature ratio, $T_s/T_p$

$\omega$ weight-flow ratio, $W_s/W_p$

Subscripts:

i ideal

p primary

s secondary

0 free stream

7 inlet to primary nozzle

8 nozzle throat station

## APPARATUS AND INSTRUMENTATION

### Nozzle Configurations and Instrumentation

The model nozzle configurations simulated the important features of a stowed thrust reverser which were expected to influence the forward thrust performance of the nozzle. The particular thrust reverser considered is shown in figure 1. Cascade boxes, which would guide the jet gases during reverse thrust operation, are built into the primary nozzle leaves. The cascade boxes are sealed from the jet gases during forward thrust operation (fig. 1(a)) by a circumferential seal. Each primary nozzle leaf has a track, which is a segment of a circular arc, attached to its outer surface. The tracks move over rollers attached to leaf support brackets which are, in turn, attached to the leaf support ring. As the leaves move aft (fig. 1(b)), the leaves close against the plug surface and the cascade boxes move downstream of the circumferential seal. In this position, the flow is turned forward by the cascades and reverse thrust is obtained. An isometric view of the primary nozzle leaves in the maximum-open position is shown in figure 1(c), and an isometric view of the leaves in the reverse thrust position is shown in figure 1(d). This thrust reverser concept requires no additional moving parts, provides a circular-arc boattail for low-drag subsonic operation, and permits the extension of cylindrical shrouds for efficient supersonic operation.

The model nozzle configurations consisted of a $10^{\circ}$ half-angle plug with two throat geometries (afterburner-on and afterburner-off) and three shrouds (one retracted and two extended). The nozzle configurations are shown installed on the wind tunnel support model in figures 2 to 5. Figure 6 is an assembly drawing of the nozzle.

Primary nozzle details are shown in figure 7. The primary nozzles simulated two forward thrust positions of the translating iris primary nozzle. The blockage of the secondary flow passage by boxes, tracks, and support brackets was simulated with

appropriately shaped protuberances on the outside of the primary nozzles.

Details of the three shrouds are shown in figure 8. One of the two extended shrouds had a smooth internal surface (fig. 4), simulating the extended shroud tested in reference 1. The other extended shroud had axial slots (fig. 5), simulating the geometry which would be required to allow the shroud to slide over the primary nozzle support brackets. Nozzle area ratios and pressure ratios for the plug nozzle with the stowed thrust reverser are listed in table I. The same information for similar configurations of the nozzle in reference 1 is listed in table II. The projected plug areas downstream of the throat (ratioed to the throat areas) for both plug nozzles are compared in table III. With the afterburner off, the configuration of reference 1 had significantly more projected plug area than that of the thrust reverser plug nozzle because in the latter case the primary nozzle leaves were translated downstream to restrict the throat area. The minimum geometric secondary flow areas (ratioed to the throat areas) for both plug nozzles are compared in table IV. The secondary flow areas for the thrust reverser plug nozzle were significantly less than that for the nozzle of reference 1. Also note that for the plug nozzle with the thrust reverser, the secondary flow area increased more rapidly than the primary flow area in going from the afterburner-off to the afterburner-on configuration. This is because the cascade boxes moved upstream of the minimum secondary flow area.

The primary and secondary total pressures and temperatures were obtained by use of total-pressure probes, static-pressure taps and thermocouples, as shown in figure 9.

## Installation in 8- by 6-Foot Supersonic Wind Tunnel

A schematic drawing of the model support system in the 8- by 6-Foot Supersonic Wind Tunnel showing the internal geometry and thrust-measuring system is shown in figure 10. The grounded portion of the model was supported from the tunnel ceiling by a vertical strut. The floating portion was cantilevered by flow tubes from external supply manifolds. The primary air bottle was supported by front and rear bearings. The secondary air passed through hollow struts at station 100.66 (255.68 cm) to the annulus formed between the primary nozzle and the shroud. The axial force of the nozzle, which included secondary and external flow effects, was transmitted to the load cell located in the nose of the model.

A static calibration of the thrust-measuring system was obtained by applying known forces to the nozzle and measuring the output of the load cell. A water-cooled jacket surrounded the load cell and maintained a constant temperature of $90^{\circ}$ F (305.6 K) to eliminate errors in the calibration due to variations in temperature from aerodynamic heating.

## PROCEDURE

Nozzle performance was obtained over a range of pressure ratios at several Mach numbers for each shroud length tested. Since tunnel static pressure was fixed at a given Mach number, the nozzle pressure ratio was varied by changing the nozzle-inlet pressure. The maximum pressure ratio at each Mach number was restricted because of the limitations of the primary air supply. The highest pressure ratio obtained was approximately 27.0 at Mach 1.97. To obtain a realistic simulation of important flight conditions, nozzle pressure ratio was varied at each Mach number around a typical schedule, shown in figure 11, for a supersonic turbojet engine. At some Mach numbers and pressure ratios close to the schedule, corrected secondary-weight-flow ratio was varied from 0 to about 15 percent.

## DATA REDUCTION

Both primary and secondary flow rates were measured by means of standard ASME flowmetering orifices located in the external supply lines. Thrust-minus-drag measurements were obtained from a load-cell readout of the axial forces acting on the floating portion of the model. Internal tare forces, determined by internal areas and measured tare pressures located as shown in figure 10, were accounted for in the thrust calculation.

The only external friction drag charged to the nozzle is that downstream of station 113.49 (288.3 cm), shown in figure 10. The friction force acting on the portion of the model between station 93.65 (237.9 cm) and 113.49 (288.3 cm) was also measured on the load cell, but it is not considered to be part of the nozzle drag. Its magnitude was estimated by using the semiempirical flat-plate mean skin friction coefficient given in figure 7 of reference 2 as a function of free-stream Mach number and Reynolds number. The coefficient accounts for variations in boundary-layer thickness and profile with Reynolds number. Measurements of the boundary-layer characteristics at the aft end of this jet exit model in the 8- by 6-Foot Supersonic Wind Tunnel are reported in reference 3 and indicate that the profile and thickness are essentially the same as those computed for a flat plate of equal length. Momentum thickness varied from 0.0221 d at Mach 0.56 to 0.0152 d at Mach 1.47. The strut wake appeared to affect only a localized region near the top of the model and resulted in a slightly lower local free-stream velocity than measured on the side and bottom of the model. Therefore, the results of reference 2 were used without correction for three-dimensional flow effects or strut interference effects. The resulting correction was applied to the load-cell force.

Reference 4 has shown that tunnel interference influences the external pressure in

the region of the nozzle when this support model is used at Mach numbers above 1.0. For this reason, no thrust data are presented for unshrouded nozzle configurations above Mach 1.0. The performance of the shrouded configurations, however, is believed to be less influenced by these disturbances since the exterior surfaces were to be more nearly cylindrical.

## RESULTS AND DISCUSSION

The measured thrust and pumping characteristics are presented in this section. Thrust characteristics are presented in terms of nozzle efficiency $(F - D)/(F_{i,p} + F_{i,s})$ and gross-thrust coefficient $(F - D)/F_{i,p}$. Pumping characteristics are presented in terms of required secondary total-pressure recovery $P_s/P_0$ and secondary total-pressure ratio $P_s/P_7$.

Nozzle efficiency is shown as a function of free-stream Mach number in figure 12. Data are shown for both the plug nozzle with the thrust reverser and a plug nozzle with a hinged iris primary flap as reported in reference 1. The pressure ratio schedule of figure 10 was used to select the data. At Mach 0 the two nozzles had similar performance. At subsonic cruise, the plug nozzle with the stowed thrust reverser had the higher performance. For subsonic cruise at Mach 0.9, the plug nozzle with the stowed thrust reverser had a nozzle efficiency of 0.923 as opposed to 0.910 for the plug nozzle of reference 1. At other power settings and Mach numbers, the plug nozzle with the thrust reverser had lower performance.

The afterburner-on geometries are almost the same for both nozzles. Yet at Mach 2.0 and $\omega\sqrt{\tau} = 0.04$, for example, the nozzle with the thrust reverser obtains a little over 1 percent less nozzle efficiency than the nozzle of reference 1. This loss in performance may result from a less efficient expansion of the secondary flow because of the proturbances in the secondary flow passage downstream of the pressure-measuring station.

Data are also shown for the afterburner-off extended shroud configurations at Mach 2.7. The data for the plug nozzle with the thrust reverser were actually taken at Mach 1.97 but at a nozzle pressure ratio of 26 and are thus representative of supersonic-cruise performance. At these conditions, the smooth shroud configuration had an efficiency of 0.965. Slotting the shroud appeared to slightly decrease the efficiency at these conditions. The data for the nozzle of reference 1 were taken at a nozzle pressure ratio of 26 but at Mach 0, and thus has no external drag of any kind. Its efficiency at these conditons was 0.983.

Figure 13 shows nozzle efficiency as a function of corrected secondary-weight-flow ratio. The efficiency of the retracted shroud configurations (figs. 13(a) and (c)) was less

sensitive to secondary weight flow than the extended shroud configuration (fig. 13(b)). Peak efficiency for all configurations of the plug nozzle with the thrust reverser occurred between 0 and 4 percent corrected secondary-weight-flow ratio. The data for the retracted shroud configuration of reference 1 indicate that its peak efficiency occurred at somewhat higher corrected secondary-weight-flow ratios.

In figure 14, gross-thrust coefficients and required secondary total-pressure recovery are presented as a function of free-stream Mach number. The pressure ratio schedule of figure 11 was again used. Slotting the extended shroud with the afterburner-off primary nozzle had little effect on gross-thrust coefficient at the lower pressure ratios shown on this figure.

The required secondary total-pressure recoveries are shown in the bottom of figure 14. For some power settings and corrected secondary-weight-flow ratios, secondary air must be supplied to the nozzle at pressures higher than free-stream total because of choking in the restricted secondary passage. At Mach 0, with the afterburner on, shroud retracted, and $\omega\sqrt{\tau} = 0.04$, the highest pressure recovery is required ($P_s = 1.2\ P_0$) because no ram pressure rise is obtained. However, with retracted shroud configurations, an $\omega\sqrt{\tau} = 0.02$ may be sufficient for cooling the primary nozzle and other engine components, even with the afterburner on. The limited data for this configuration and power setting with $\omega\sqrt{\tau} = 0.02$ show that significantly lower pressure recoveries would be required. Also, at Mach 1.2, if the shroud is maintained in the retracted position, an $\omega\sqrt{\tau} = 0.04$ could be obtained with a secondary total-pressure recovery of 0.95. At a higher Mach number, possibly 1.4, the shroud could be extended, and an $\omega\sqrt{\tau} = 0.04$ could be obtained with a secondary total-pressure recovery of 0.97.

Gross-thrust coefficients and secondary total-pressure ratios are presented as functions of nozzle pressure ratio in figure 15. The data for the afterburner-off configurations are presented in figures 15(a) to (c) and the data for the afterburner-on configurations are presented in figures 15(d) and (e).

The two flagged symbols in the top part of figure 15(a) indicate that these points were obtained by extrapolating the gross-thrust coefficient from an $\omega\sqrt{\tau} = 0.03$ to $\omega\sqrt{\tau} = 0.02$ at the indicated nozzle pressure ratios. In figures 15(a) to (e), typical external flow effects on nozzle gross-thrust coefficient are shown. By comparing figures 15(b) and (c), it appears that the extended smooth shroud configuration has higher gross-thrust coefficients than the extended slotted shroud configuration above a nozzle pressure ratio of 15. In the bottom parts of these figures the secondary total-pressure ratios required for the plug nozzle with the stowed thrust reverser are compared to secondary total-pressure ratios required by the plug nozzle of reference 1. As would be expected, a larger secondary total-pressure ratio is required for the plug nozzle with the thrust reverser because of the smaller secondary flow passages upstream of

the primary nozzle (table IV). A flattening of the curve at the higher pressure ratios indicates choking of the secondary flow.

Gross-thrust coefficients and secondary total-pressure ratios are presented as functions of corrected secondary-weight-flow ratio in figure 16. The data for the afterburner-off configurations are presented in figures 16(a) to (c) and the data for the one afterburner-on configuration where $\omega\sqrt{\tau}$ was varied are presented in figure 16(d). For $\omega\sqrt{\tau} = 0$ (and thus $F_{i,s} = 0$), it is possible to directly compare the gross-thrust coefficients of the nozzle having the stowed thrust reverser with the nozzle efficiencies in reference 1. For the afterburner-off retracted-shroud configurations (top part of fig. 16(a)), the plug nozzle with the stowed thrust reverser had a higher value of gross-thrust coefficient at Mach 0.9 and a nozzle pressure ratio of 3.82. This effect may be caused by a reduced boattail drag resulting from the circular-arc boattail. At Mach 0.9 and a nozzle pressure ratio of 5.62 (conditions where boattail drag is a smaller part of the ideal thrust), the plug nozzle of reference 1 had a slightly higher gross-thrust coefficient. The better performance of the reference 1 nozzle may be due to higher boattail pressures resulting from the more blunt primary nozzle external surface and its close proximity to the underexpanded primary jet. The secondary total-pressure ratio curves for all configurations (bottom parts of figs. 16(a) to (d)) agree fairly well with theoretical values assuming choked secondary flow in the minimum geometric secondary flow area.

The gross-thrust coefficients for the afterburner-off, extended-shroud configuration (top parts of figs. 16(b) and (c)) were measured at a free-stream Mach number of 1.97 but at a nozzle pressure ratio of about 26 and are indicative of supersonic-cruise gross-thrust coefficients. At $\omega\sqrt{\tau} = 0$, the gross-thrust coefficient for the plug nozzle with the stowed thrust reverser is about 2.3 percentage points less than that for the plug nozzle of reference 1. This could be due to the smaller projected plug area (1.122 $A_8$ as opposed to 1.210 $A_8$), and a shorter internal expansion length (0.523 d as opposed to 0.618 d) which would provide less containment of the initial primary flow expansion. A method of characteristics analysis of the two configurations indicates that a difference in gross-thrust coefficient of at least 1 percentage point could be expected because of the geometric differences and suggests that the afterburner-off throat station of the plug nozzle with the thrust reverser should be moved upstream. If the afterburner-off throat station were moved to the same axial location as the reference 1 nozzle, the afterburner-on throat station would also move upstream to the curved portion of the plug. The movement could be minimized by increasing the primary nozzle curvature at the expense of some increase in the boattail angle at the trailing edge of the primary nozzle leaves. Comparison of the performance in figures 16(b) and (c) shows that slotting the shroud decreased the gross-thrust coefficient from 0.3 to 0.5 percentage point at a nozzle pressure ratio of 26.0.

In figure 16(d) the afterburner-on, retracted-shroud configuration of the plug nozzle with the thrust reverser is shown to have a slightly higher gross-thrust coefficient at $\omega\sqrt{\tau} = 0$ than the nozzle of reference 1. Projected plug areas for these configurations are approximately equal (0.891 $A_8$ and 0.867 $A_8$) and thus the primary nozzle shape, both external and internal, may account for the performance difference.

## SUMMARY OF RESULTS

A wind tunnel model of a $10^{\circ}$ conical plug nozzle with a stowed thrust reverser was evaluated over a range of Mach numbers from 0 to 2.0 at appropriate nozzle pressure ratios. Room-temperature air was used as the primary and secondary fluid. Two primary nozzle areas and two shroud lengths were used during the tests. The small primary area simulated afterburner-off operation at subsonic speeds when combined with the short shroud, and supersonic-cruise operation when combined with the long shroud. The larger primary nozzle area simulated a throat geometry which would exist at afterburner-on power settings. Nozzle gross-thrust coefficients and pumping characteristics were measured and compared to those obtained from a hinged iris primary plug nozzle without a reverser (ref. 1). The important results are summarized as follows:

1. The nozzle had a high gross-thrust coefficient at subsonic cruise (0.96 at $M_0 = 0.85$ and $\omega\sqrt{\tau} = 0.02$). At a Mach number of 1.97 and a nozzle pressure ratio of 26 with no secondary flow, the nozzle gross-thrust coefficient was 0.950, which was 2.3 percentage points less than that for a hinged iris primary plug nozzle without a thrust reverser. It also had a lower efficiency at all acceleration power settings.

2. The stowed thrust reverser restricted the secondary flow to the extent that it would be impossible to obtain a corrected secondary-weight-flow ratio of 0.04 from the free stream below Mach 1.1. However, a corrected secondary-weight-flow ratio of 0.02 could be obtained from a free-stream source at Mach numbers above 0.40. Thus, if the retracted shroud configurations can be cooled with a corrected secondary-weight-flow ratio of 0.02 (exclusive of plug cooling requirements), and if the shroud is extended only above Mach 1.4, it may be possible to obtain the secondary air from a free-stream source at all flight conditions above Mach 0.4.

3. Slotting the shroud to provide for translation over the primary nozzle support brackets had little effect on nozzle performance.

Lewis Research Center,
National Aeronautics and Space Administration,
Cleveland, Ohio, June 16, 1970,
720-03.

# REFERENCES


1. Bresnahan, Donald L.: Experimental Investigation of a $10^{o}$ Conical Turbojet Plug Nozzle With Iris Primary and Translating Shroud at Mach Numbers From 0 to 2.0. NASA TM X-1709, 1968.

2. Smith, K. G.: Methods and Charts for Estimating Skin Friction Drag in Wind Tunnel Tests With Zero Heat Transfer. Rep. ARC-CP-824, Aeronautical Research Council, Great Britain, 1965. (Available from DDC as AD-487132.)

3. Harrington, Douglas E.: Jet Effects on Boattail Pressure Drag of Isolated Ejector Nozzles at Mach Numbers From 0.60 to 1.47. NASA TM X-1785, 1969.

4. Blaha, Bernard J.; and Bresnahan, Donald L.: Wind Tunnel Installation Effects on Isolated Afterbodies at Mach Numbers From 0.56 to 1.5. NASA TM X-52581, 1969.

TABLE I. - PRESSURE RATIOS AND AREA RATIOS FOR PLUG NOZZLE WITH THRUST REVERSER

[Overall design pressure ratio, $P_7/p_0$: afterburner off, 27.55; afterburner on, 15.92.]

| Shroud length to diameter ratio | Afterburner off | | Afterburner on | |
|---|---|---|---|---|
| | Internal expansion pressure ratio | Internal area ratio | Internal expansion pressure ratio | Internal area ratio |
| Retracted: | | | | |
| -0.235 | ----- | ---- | 1.89 | 1.00 |
| -0.332 | 1.89 | 1.00 | ----- | ---- |
| Extended: | | | | |
| 0.618 | ----- | ---- | 12.50 | 2.19 |
| 0.523 | 21.89 | 3.06 | ----- | ---- |

TABLE II. - PRESSURE RATIOS AND AREA RATIOS FOR PLUG NOZZLE REPORTED IN REFERENCE 1

[Overall design pressure ratio, $P_7/p_0$: afterburner off, 26.3; afterburner on, 15.1.]

| Shroud length to diameter ratio | Afterburner off | | Afterburner on | |
|---|---|---|---|---|
| | Internal expansion pressure ratio | Internal area ratio | Internal expansion pressure ratio | Internal area ratio |
| Retracted, -0.235 | 1.89 | 1.0 | 1.89 | 1.0 |
| Extended, 0.618 | 21.10 | 2.99 | 11.93 | 2.13 |

TABLE III. - RATIO OF PROJECTED PLUG AREA DOWNSTREAM OF THROAT TO THROAT AREA

| | Plug nozzle with thrust reverser | Nozzle of reference 1 |
|---|---|---|
| Afterburner off | 1.122 | 1.210 |
| Afterburner on | .891 | .867 |

TABLE IV. - RATIO OF MINIMUM GEOMETRIC SECONDARY FLOW AREA TO GEOMETRIC PRIMARY NOZZLE FLOW AREA

| | Plug nozzle with thrust reverser | Nozzle of reference 1 |
|---|---|---|
| Afterburner off | 0.108 | 0.332 |
| Afterburner on | .136 | .238 |

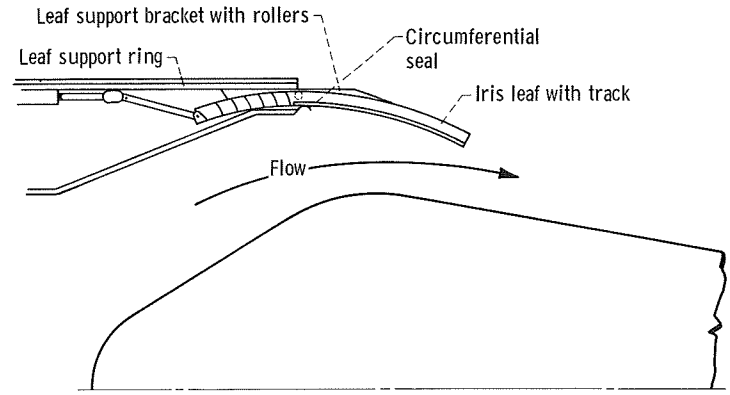


(a) Forward thrust.

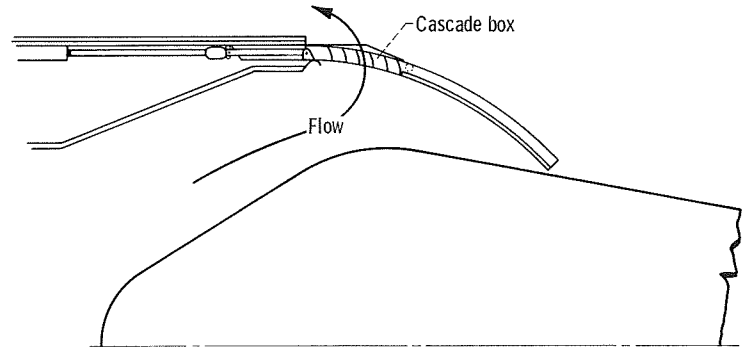


(b) Reverse thrust.

CD-10842-28

Figure 1. - Thrust reverser for plug nozzle.

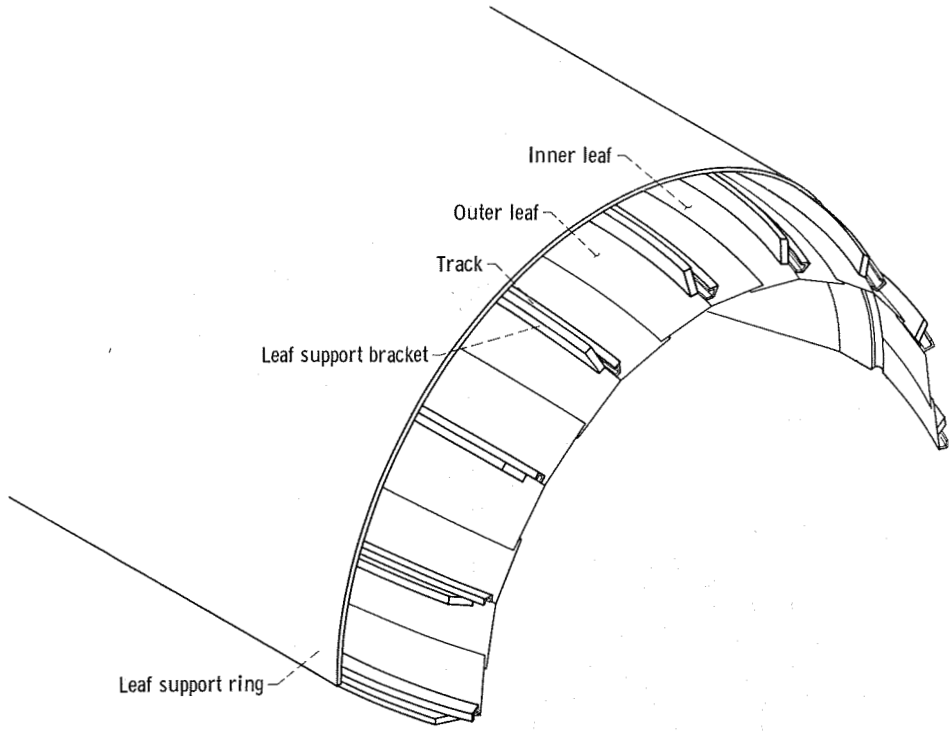


(c) Primary nozzle leaves in maximum open position.

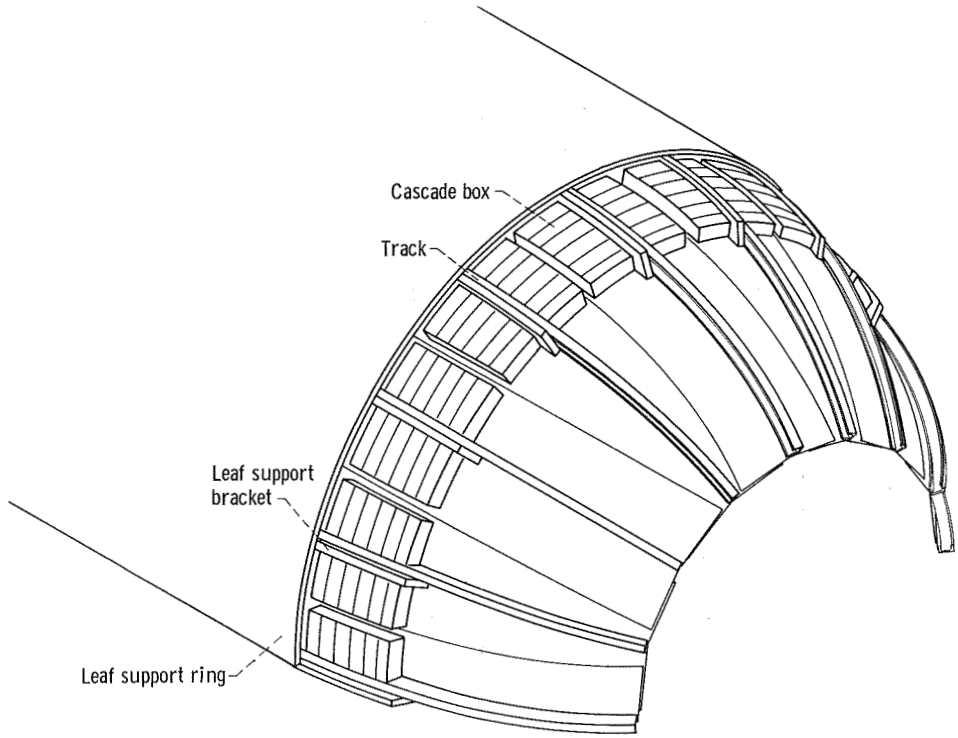


(d) Primary nozzle leaves in reverse thrust position. CD-10843-28

Figure 1. - Concluded.

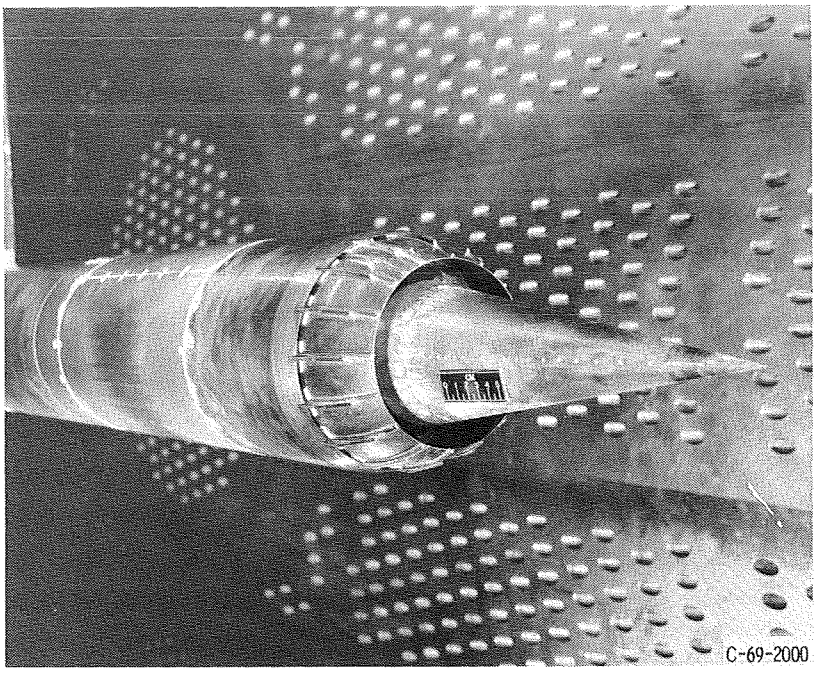


Figure 2. - Afterburner-off, retracted shroud configuration.

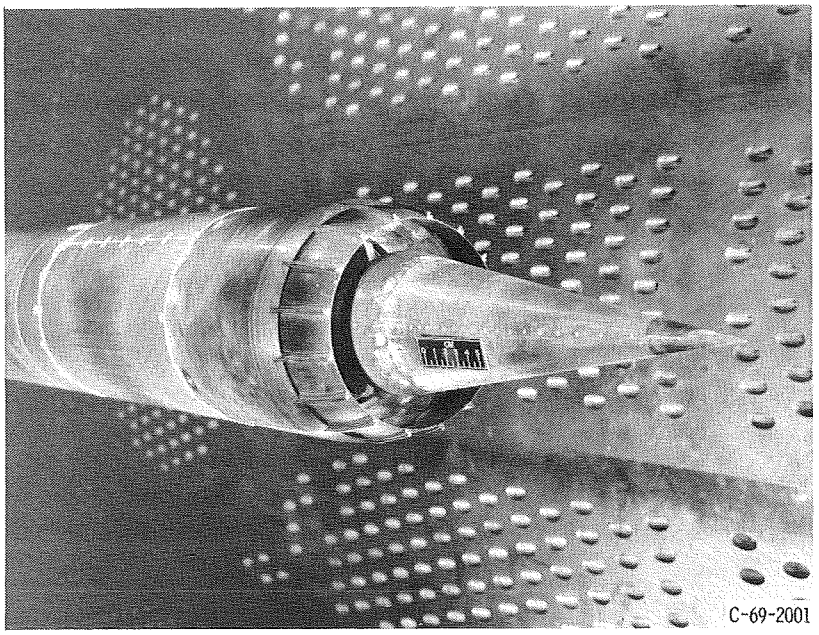


Figure 3. - Afterburner-on, retracted shroud configuration.

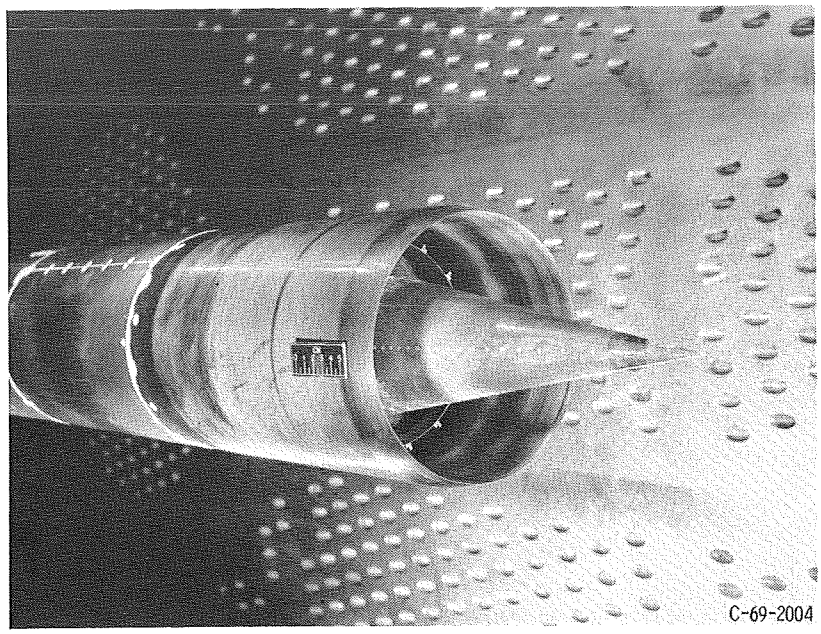


Figure 4. - Extended smooth shroud configuration.

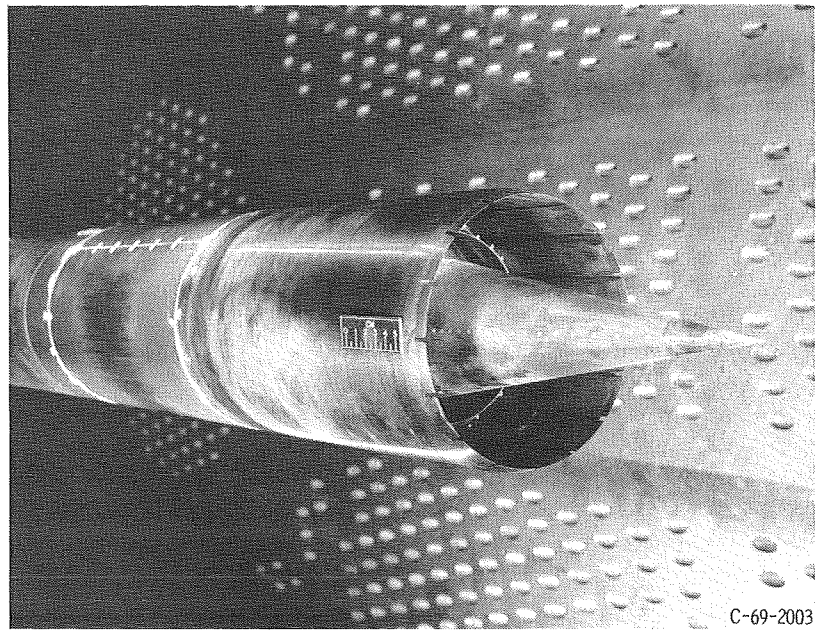


Figure 5. - Extended slotted shroud configuration.

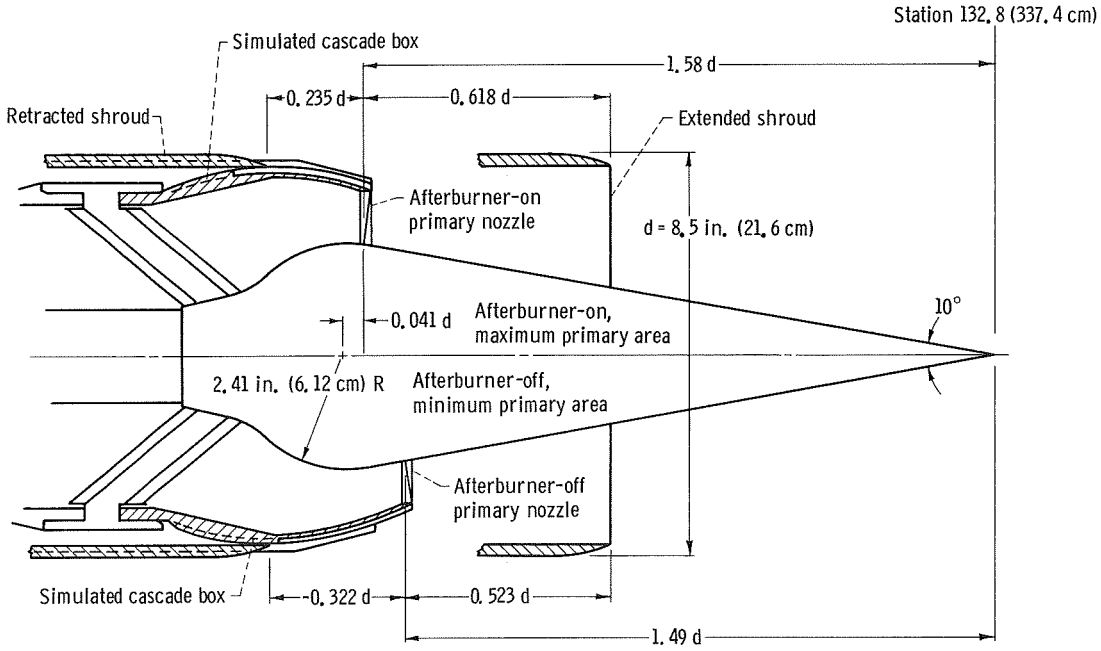


Figure 6. - Assembly of plug nozzle.

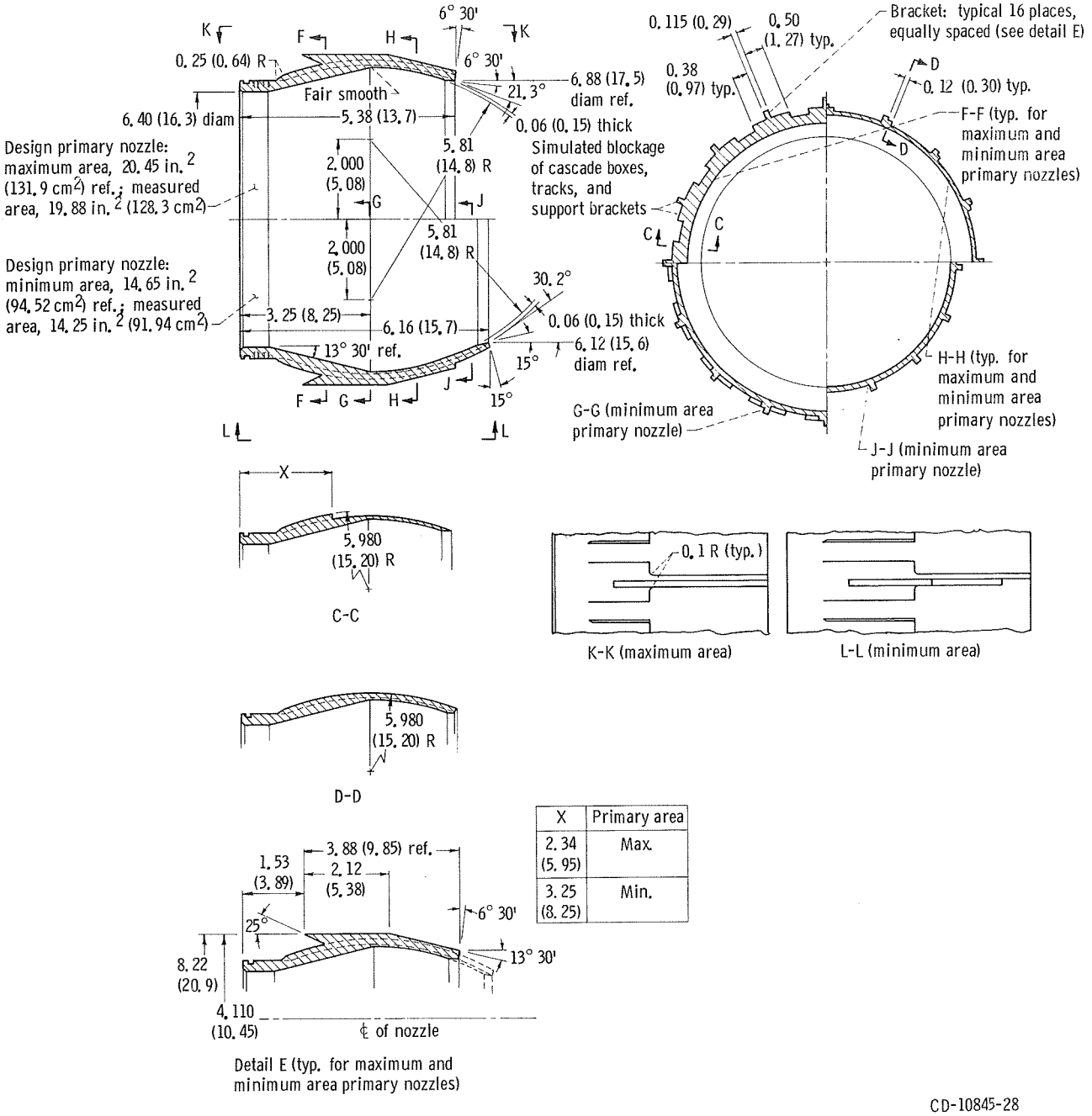


| X | Primary area |
|---|---|
| 2. 34 (5. 95) | Max. |
| 3. 25 (8. 25) | Min. |

CD-10845-28

Figure 7. - Primary nozzle details. (All dimensions are in inches (cm).)

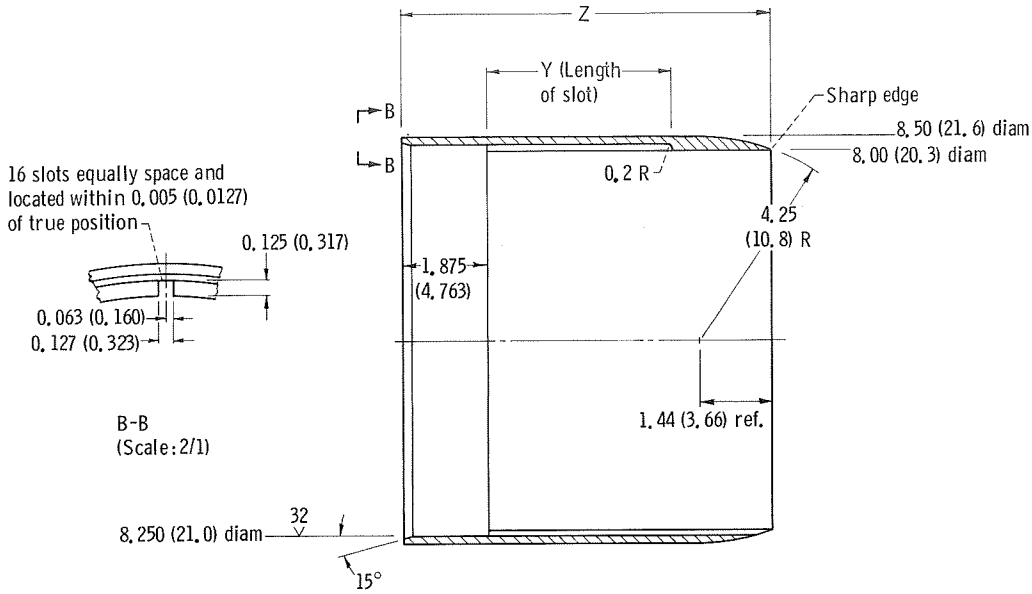


| Shroud configuration | Z | | Y | |
|---|---|---|---|---|
| | in. | cm | in. | cm |
| Retracted | 7.78 | 19.8 | 5.9 | 15.0 |
| Extended smooth | 15.03 | 38.15 | 6.9 | 17.5 |
| Extended slotted | 15.03 | 38.15 | 13.2 | 33.4 |

CD-10846-28

Figure 8. - Shroud details. (All dimensions are in inches (cm).)

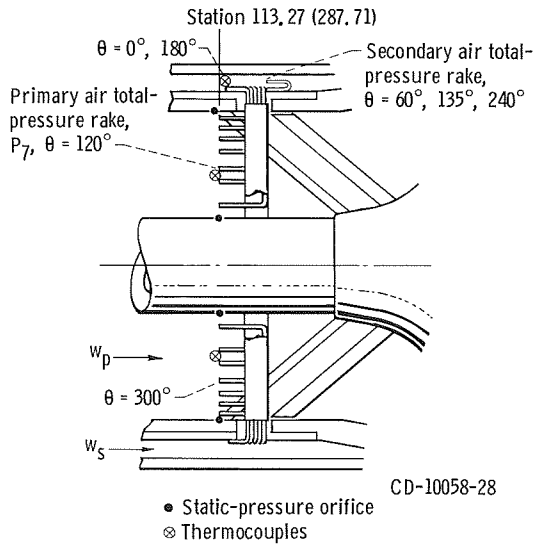


Figure 9. - Primary and secondary instrumentation.

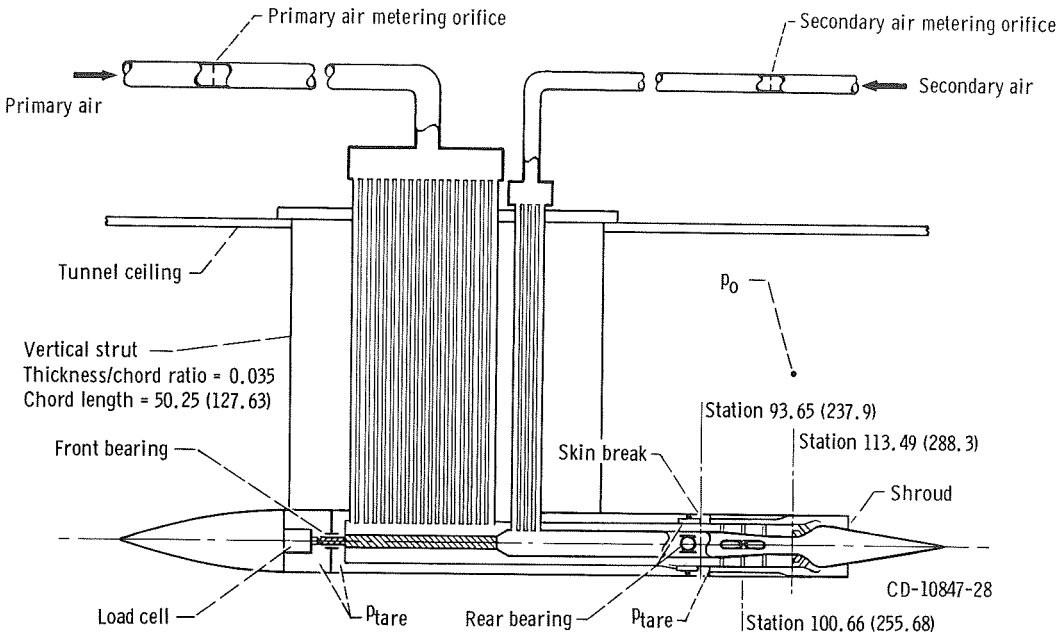


Figure 10. - Schematic view of nozzle support model and air supply systems for 8- by 6-Foot Supersonic Wind Tunnel. (Dimensions are in inches (cm).)

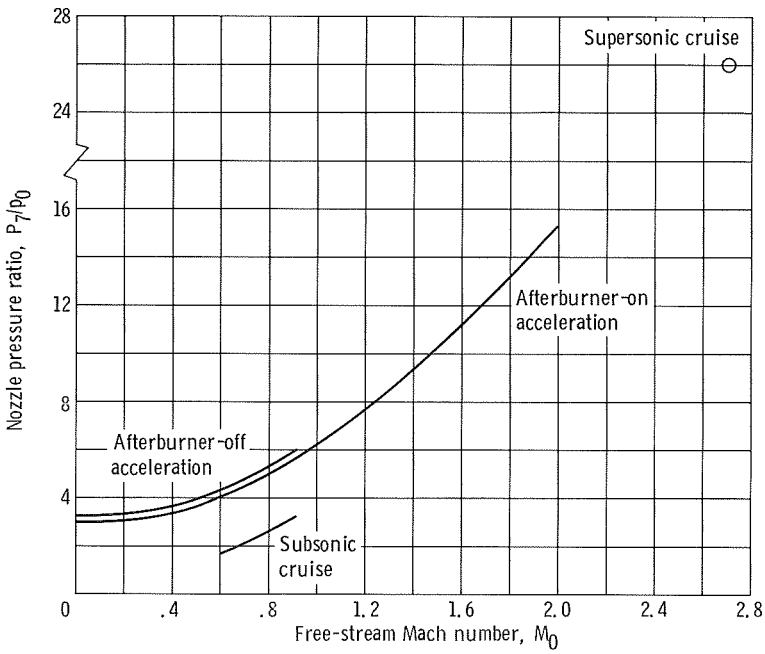


Figure 11. - Schedule of nozzle pressure ratio with free-stream Mach number for four simulated power settings.

| Afterburner | Shroud configuration | Corrected secondary-weight-flow ratio, $\omega\sqrt{\tau}$ |
|---|---|---|
| □ On | Retracted | 0.04 |
| ○ Off | Retracted | .02 |
| △ On | Extended, smooth | .04 |
| ◇ Off | Extended, smooth | .02 ($M_0$ = 1.97; $P_7/p_0$ = 26) |
| ◊ Off | Extended, slotted | .02 ($M_0$ = 1.97; $P_7/p_0$ = 26) |
| ◆ Off | Extended, smooth | .02 ($M_0$ = 0; $P_7/p_0$ = 26) |

Flagged symbols indicate $P_s < p_0$ and $F_{i,s} \equiv 0$
Solid symbols indicate ref. 1 data

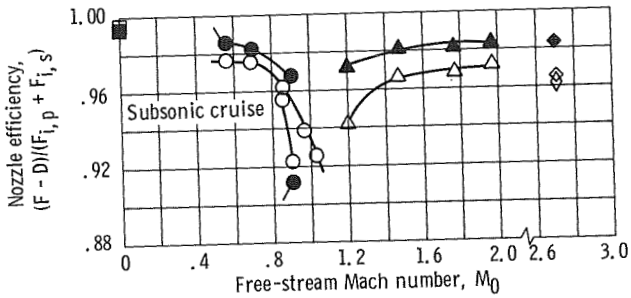


Figure 12. - Comparison of efficiency of plug nozzle having a stowed thrust reverser with efficiency of plug nozzle of reference 1.

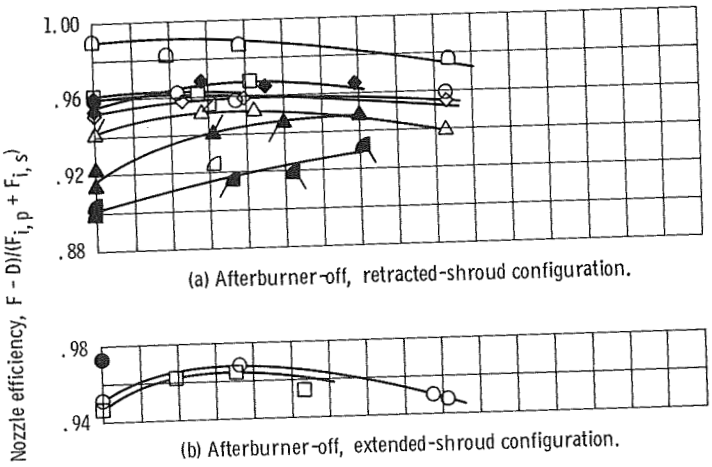


| Free-stream Mach number, $M_0$ | Nozzle pressure ratio, $P_7/p_0$ |
|---|---|
| □ 0 | 3.29 |
| ○ .85 | 5.26 |
| □ .85 | 3.58 |
| ◁ .85 | 2.87 |
| ◇ .90 | 5.62 |
| ◆ .90 | 6.00 |
| △ .90 | 3.82 |
| ▲ .90 | 4.03 |
| ◁ .90 | 3.21 |
| ◢ .90 | 3.25 |

Solid symbols denote data from ref. 1
Flagged symbols indicate $P_s < p_0$ and $F_{i,s} \equiv 0$

| | | |
|---|---|---|
| ○ | 1.97 | 26.3 (Smooth shroud) |
| □ | 1.97 | 26.6 (Slotted shroud) |

| | | |
|---|---|---|
| ◇ | 0 | 3.26 |
| ○ | .86 | 6.11 |
| □ | .91 | 5.64 |

Figure 13. - Variation of nozzle efficiency with corrected secondary-weight-flow ratio.

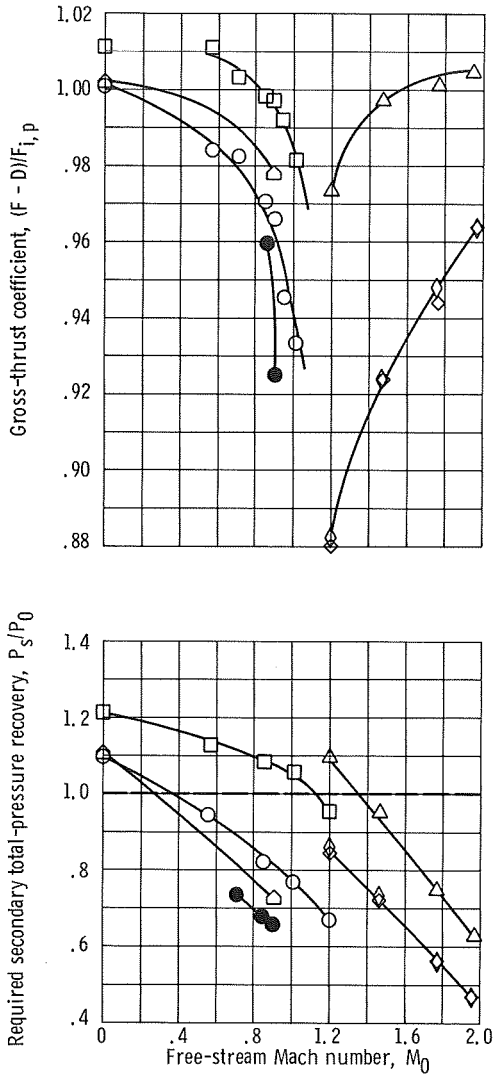


| Afterburner | Shroud configuration | Corrected secondary-weight-flow ratio, $\omega\sqrt{\tau}$ |
|---|---|---|
| On | Retracted | 0.04 |
| On | Retracted | .02 |
| Off | Retracted | .02 |
| On | Extended, smooth | .04 |
| Off | Extended, smooth | .02 |
| Off | Extended, slotted | .02 |

Open symbols denote acceleration power settings
Solid symbols denote subsonic-cruise power settings

Figure 14. - Nozzle performance over flight Mach number range.

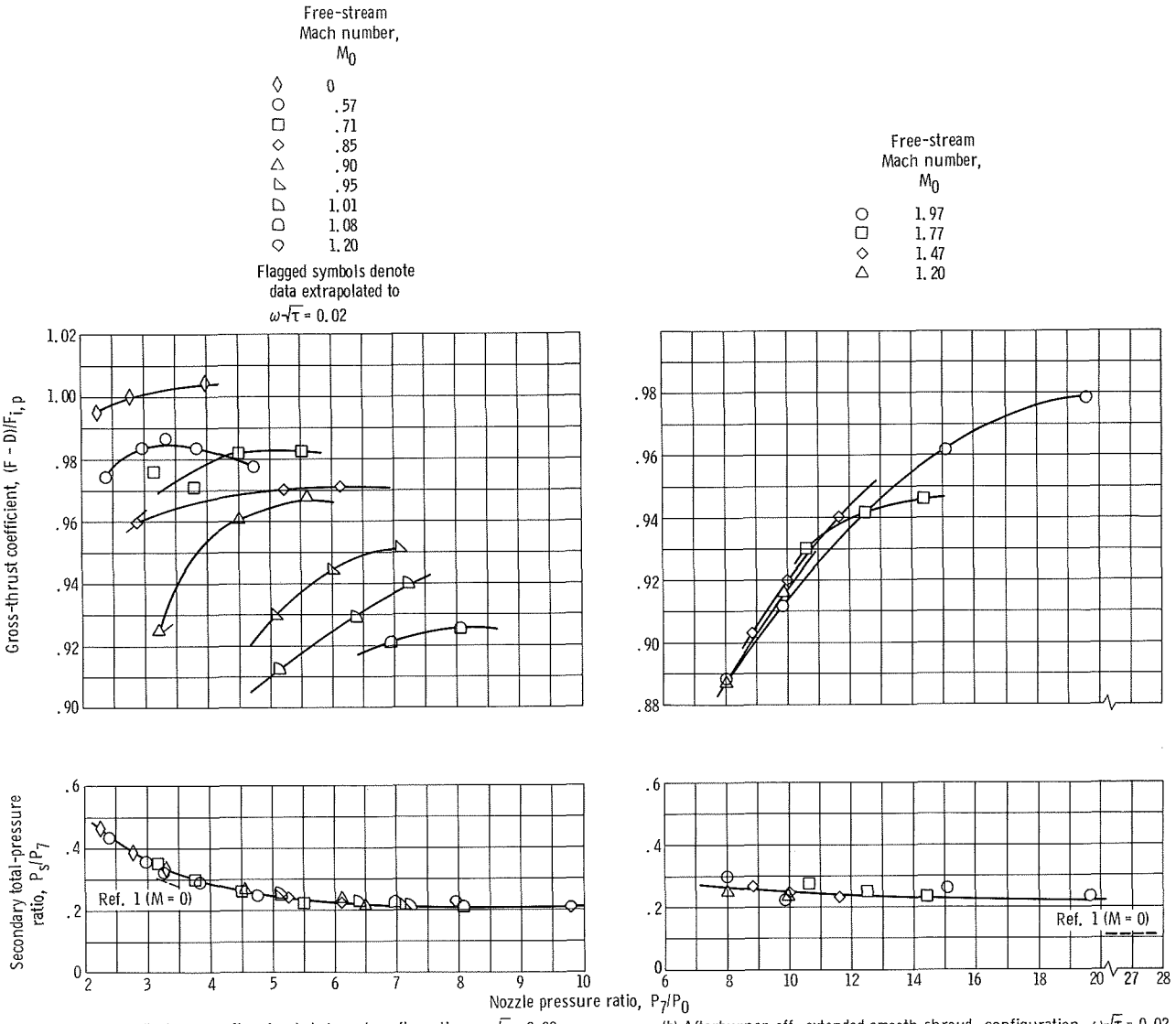


(a) Afterburner-off, retracted shroud configuration; $\omega\sqrt{\tau} = 0.02$.

(b) Afterburner-off, extended smooth shroud, configuration; $\omega\sqrt{\tau} = 0.02$.

Figure 15. - Nozzle performance for various nozzle configurations and corrected secondary-weight-flow ratios $\omega\sqrt{\tau}$ of 0.02 and 0.04.

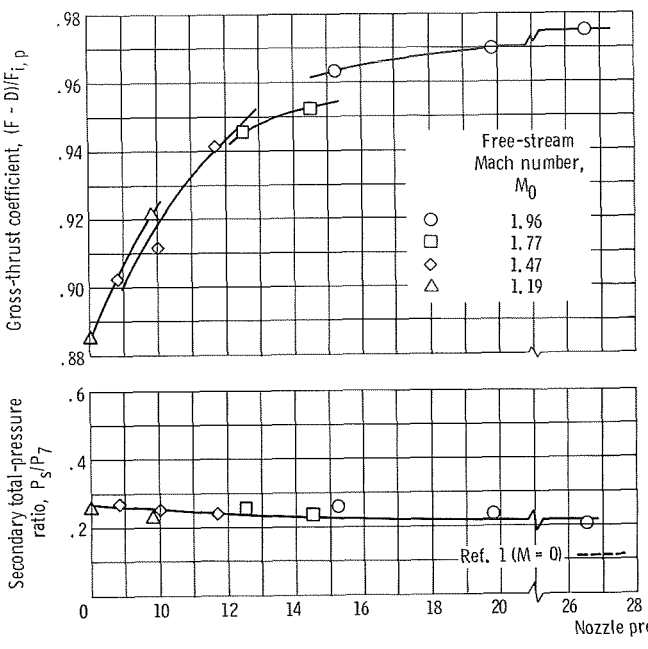


(c) Afterburner-off, extended slotted shroud configuration; $\omega\sqrt{\tau} = 0.02$.

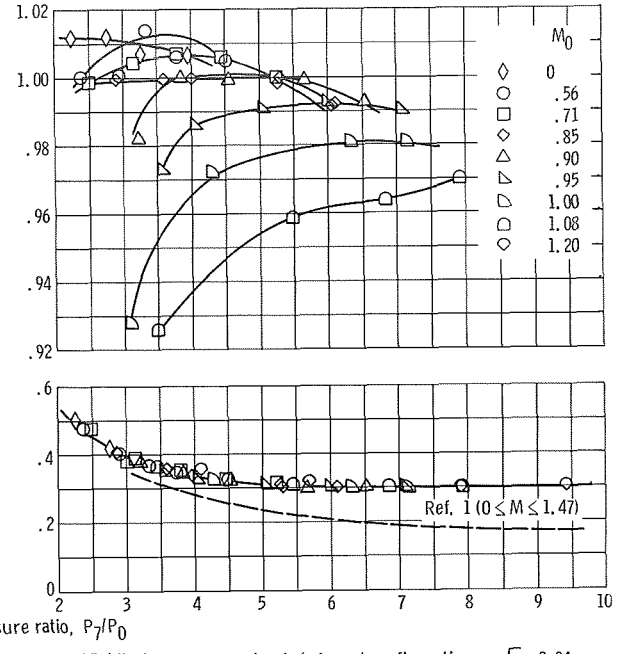


(d) Afterburner-on, retracted shroud configuration; $\omega\sqrt{\tau} = 0.04$.

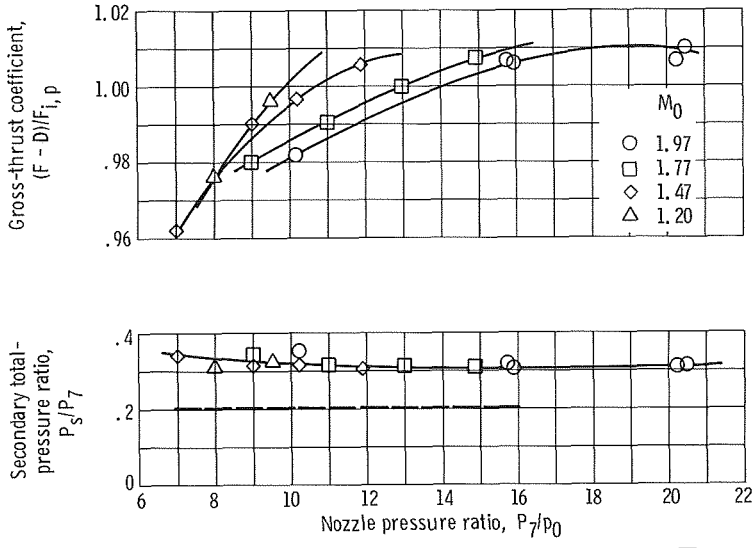


(e) Afterburner-on, extended smooth shroud configuration; $\omega\sqrt{\tau} = 0.04$.

Figure 15. - Concluded.

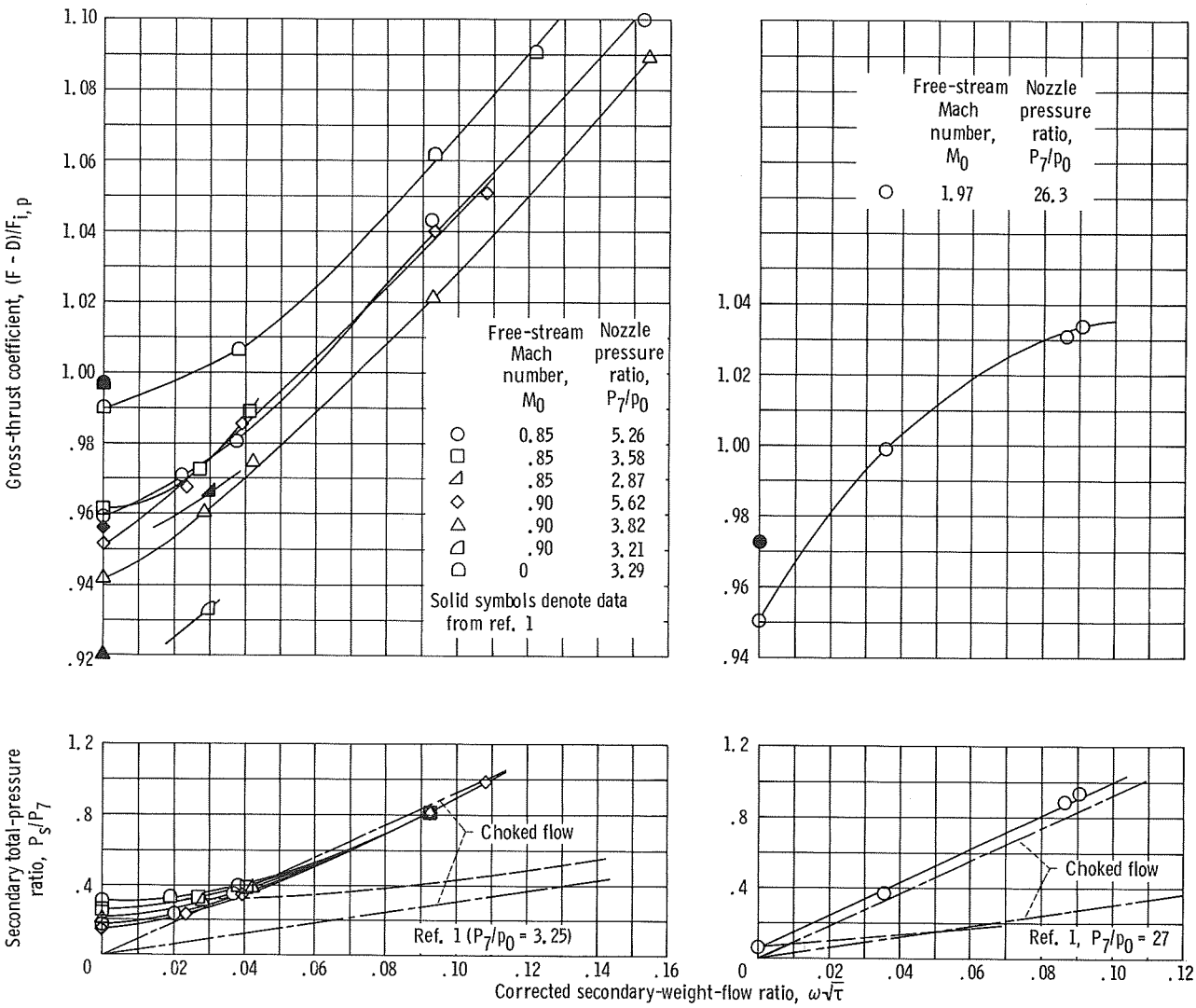


(a) Afterburner-off, retracted shroud configuration.

(b) Afterburner-off, extended smooth shroud configuration.

Figure 16. - Effect of corrected secondary-weight-flow ratio on nozzle performance.

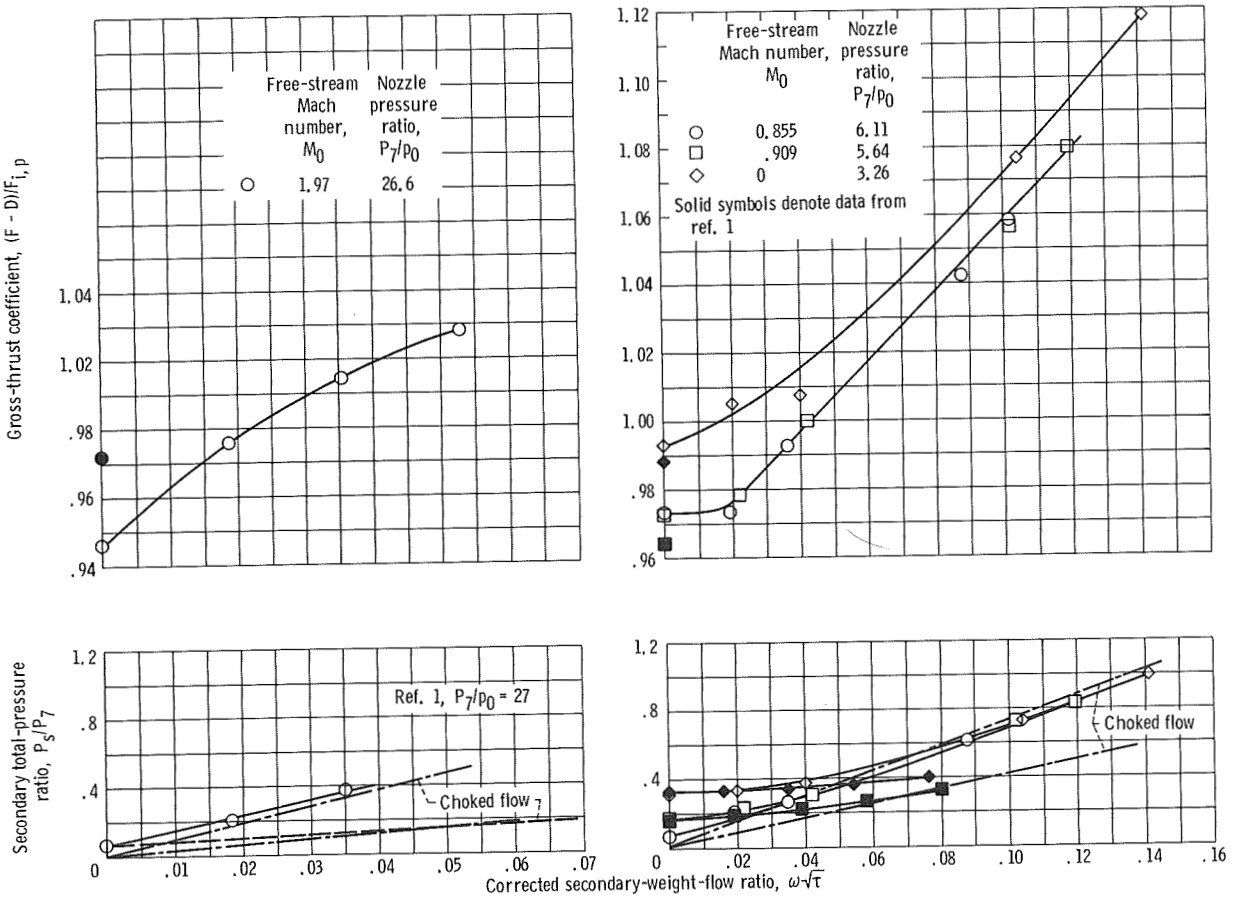


(c) Afterburner-off, extended slotted shroud configuration.

(d) Afterburner on, retracted shroud configuration.

Figure 16. - Concluded.

NATIONAL AERONAUTICS AND SPACE ADMINISTRATION
WASHINGTON, D.C. 20546

OFFICIAL BUSINESS

FIRST CLASS MAIL

POSTAGE AND FEES PAID
NATIONAL AERONAUTICS AND
SPACE ADMINISTRATION

POSTMASTER: If Undeliverable (Section 158 Postal Manual) Do Not Return

*"The aeronautical and space activities of the United States shall be conducted so as to contribute . . . to the expansion of human knowledge of phenomena in the atmosphere and space. The Administration shall provide for the widest practicable and appropriate dissemination of information concerning its activities and the results thereof."*

—NATIONAL AERONAUTICS AND SPACE ACT OF 1958

# NASA SCIENTIFIC AND TECHNICAL PUBLICATIONS

TECHNICAL REPORTS: Scientific and technical information considered important, complete, and a lasting contribution to existing knowledge.

TECHNICAL NOTES: Information less broad in scope but nevertheless of importance as a contribution to existing knowledge.

TECHNICAL MEMORANDUMS: Information receiving limited distribution because of preliminary data, security classification, or other reasons.

CONTRACTOR REPORTS: Scientific and technical information generated under a NASA contract or grant and considered an important contribution to existing knowledge.

TECHNICAL TRANSLATIONS: Information published in a foreign language considered to merit NASA distribution in English.

SPECIAL PUBLICATIONS: Information derived from or of value to NASA activities. Publications include conference proceedings, monographs, data compilations, handbooks, sourcebooks, and special bibliographies.

TECHNOLOGY UTILIZATION PUBLICATIONS: Information on technology used by NASA that may be of particular interest in commercial and other non-aerospace applications. Publications include Tech Briefs, Technology Utilization Reports and Notes, and Technology Surveys.

*Details on the availability of these publications may be obtained from:*

SCIENTIFIC AND TECHNICAL INFORMATION DIVISION

NATIONAL AERONAUTICS AND SPACE ADMINISTRATION

Washington, D.C. 20546